

BIOLOGICAL AND PHOTOCATALYTIC POTENTIAL OF PHYTOCHEMICALLY SYNTHESIZED ZINC OXIDE NANOPARTICLES

ASMA KHAN

MS student, Institute of Biotechnology and Microbiology (IBM), Bacha Khan University, Charsadda, Pakistan. Email: asmakhaan38@gmail.com, Orcid Id: 0009-0003-1764-5075

Dr. FARHAD ALI

Assistant Professor, Institute of Biotechnology & Microbiology, Bacha Khan University, Charsadda, Pakistan. Corresponding Author Email: drfarhad@bkuc.edu.pk, Orcid Id: 0000-0002-8649-558X

TAHIR SALAM

MS student, Institute of Biotechnology and Microbiology (IBM), Bacha Khan University, Charsadda, Pakistan. Email: tahirsalam.biotech@bkuc.edu.pk, Orcid Id: 0000-0003-4627-5758

FAWAD ALI

Institute of Biotechnology & Microbiology, Bacha Khan University, Charsadda, Pakistan.
Email: fawadansi@gmail.com

Abstract

Background/aim: Aqueous phytochemical extract of *Spirogyra* (Algae) was used in the present work as a reducing and capping agent to synthesize zinc oxide nanoparticles (NPs). **Methodology and results:** The phytochemical synthesis of nanoparticles was confirmed using UV-Vis Spectrophotometer, showing an absorption peak at the 280nm wavelength range. Fourier transform infrared spectroscopy (FTIR) evaluated the role of active phytochemicals derived from *Spirogyra* extract. Scanning electron microscopy (SEM) identified irregular and homogenous morphology, and the XRD identified the crystalline structure of ZnO nanoparticles with an average size of 52.96 nm. EDX analysis identified the elemental composition of ZnO nanoparticles. Furthermore, the biological activities of the phytochemically synthesized NPs revealed an excellent therapeutic potential. The synergistic bactericidal effect of the NPs and antibiotics was assessed against selected pathogenic bacterial strains. The highest inhibition activity was observed against *K. pneumonia* and *B. subtilis* with an inhibition zone of 30 ± 0.21 and 30 ± 0.26 , respectively. DPPH (2, 2-diphenyl-1-picryl-hydrazine) assay demonstrated ZnO NPs' free radical scavenging ability (81.10 ± 0.26) at 100 $\mu\text{g/ml}$. The biocompatible ZnO nanoparticles demonstrated outstanding antileishmanial efficacy against amastigotes and promastigotes ($79\% \pm 0.65$ and $80\% \pm 0.155$, respectively) compared to the standard treatment of Amphotericin B (88 and 94% at 100 $\mu\text{g/ml}$). Biogenic Zinc oxide nanoparticles were used as a catalyst for removing organic dyes, methylene blue and Methyl red, with an efficiency of 84% and 95%, respectively. **Conclusion:** The finding of this study suggests that spirogyra extract-mediated synthesis of ZnO nanoparticles is a promising approach towards sustainable and eco-friendly nanotechnology and may be further evaluated for in-situ and commercial applications.

Keywords: Spirogyra phytochemicals, ZnO-NPs, Bactericidal activity, antioxidant activity, antileishmanial, environmental application of nanoparticles

1. INTRODUCTION

Nanotechnology is a highly regarded subject in the recent material field of science. This technology has a wide and unique application, including revolutionary fabric materials, food manufacturing, agricultural production, and advanced medical approaches (Pramanik, et al. 2020). These nanostructures display novel and significantly increased

physicochemical and biological characteristics and functions (Asha and Narain 2020). Nanoparticles (NPs) have comparatively larger surface areas than macro-sized particles because of their nanoscale size (Singh and Katare 2019). They have size-related characteristics that differ significantly from bulk materials (Zhang, et al. 2018). Compared to their predecessors, NPs have bigger structures due to their very small size. Metal oxides are especially intriguing, scientifically and technologically, among all the materials with nanoscale diameters. Due to a wide range of possible applications in biological, optical, and electrical sectors, metal oxide NPs research is now a hot topic in science (Cai, et al. 2021; Chiang, et al. 2020; Tyagi, et al. 2020). Physical methods have the advantages of high speed and no toxic chemicals, purity, uniform size, and shape, but they also have the disadvantages of low productivity, high cost, radiation exposure, high energy, temperature, and pressure requirements, less thermal stability, high waste, high dilution, difficult size, shape, and less stability. While in the chemical synthesis methods, various carcinogenic solvents were used. Biomolecules and green synthesis are often utilized for the production and fabrication of nanoparticles. Biological approaches are simple, easy, and ecologically acceptable, and the nanoparticles produced are harmless and biocompatible. Changing the concentration of reducing and stabilizing agents, temperature, and pH can generate nanoparticles with defined size and structure (Jeyaraj, et al. 2019; Zhang, et al. 2016). Techniques for generating nanoparticles utilizing natural products as capping and reducing molecules, such as vitamins, sugars, plant extracts, biologically friendly polymers, and microbes, are appealing for nanotechnology.

Zinc oxide is a biocompatible and very affordable crystalline inorganic semiconductor. Zinc oxide-based nanomaterials have commanded attention in recent years and are widely used in a variety of environmental and biological applications (Shafey 2020; Soto-Robles, et al. 2019; Thi, et al. 2020). *Spirogyra* is a rich source of active phytochemicals such as carbohydrates, carotenoids, polysaccharides, proteins, vitamins, and secondary metabolites (Chanda, et al. 2010; Mohamed, et al. 2012). The active chemicals found in *spirogyra* have also been proven to have therapeutic qualities that may be employed in conventional and alternative treatments (Zuercher, et al. 2006). In the present study, the phytochemicals in *spirogyra* extract were used as reducing and capping agents for synthesizing ZnO nanoparticles.

2. EXPERIMENTAL METHODOLOGIES

2.1. Extract preparation

The aqueous extract was prepared by extracting 10 g of the sun-dried *Spirogyra* powder through Soxhlet apparatus. The sample (10 g) was placed into a thimble with 100 ml sterile distilled water in a solvent flask at 60°C for 5hrs. The extract was filtered and then stored at 5°C for further experiments.

2.2. Biosynthesis of ZnO NPs

The zinc oxide nanoparticles were synthesized by adding 70ml of 0.1mM zinc nitrate solution into 30ml *spirogyra* aqueous extract on continuous stirring at room temperature

for 18 hours. The reaction mixture was centrifuged, the supernatant removed, and the pellet was collected. The pellet was isolated and washed three times with deionized double distilled water, followed by washing with 70% ethanol to remove any contaminants, followed by drying in an incubator for 2 hrs at 40°C.

2.3. Characterization of biogenic ZnO NPs

Various characterizations, i.e., UV, FTIR, SEM, TEM, XRD, and EDX, were carried out to determine the physic-chemical and morphological characteristics of synthesized ZnO NPs.

2.4. Biological activities

2.4.1. Biocompatibility against (Human) RBCs

The biosafety of biosynthesized ZnO-NPs was evaluated using a hemolytic test of RBCs. Fresh blood samples were collected from healthy individuals in EDTA (Ethylene di-amine tetra acetic acid) tubes to avoid clotting and centrifuged at 14,000 rpm. The suspension was made by adding 200µl fresh RBCs of 9.8ml potassium buffered saline (PBS) solution by gentle shaking. Erythrocyte suspensions and NPs solution were mixed in different concentrations in Eppendorf tubes and incubated for 1 hour at 35°C, then centrifuged at 10,000 rpm for 10 minutes. DMSO (Dimethyl sulfoxide) and Triton X-100 were negative and positive controls. The following formula was used to calculate the percentage hemolysis of RBCs:

$$(\%) \text{ Hemolysis} = \left(\frac{\text{sampleAb} - \text{negativecontrolAb}}{\text{PositivecontrolAb} - \text{NegativecontrolAb}} \right) \times 100$$

2.4.2. Antibacterial Assay by Disc Diffusion Method

Disc diffusion method was carried out to examine the antibacterial ability of biologically synthesized ZnO-NPs. The tested strains for the antimicrobial assay included, *Acetobacter*, *B. Subtilis*, *Klebsiella pneumonia*, *P. Aeruginosa*, and *P. Voulgaris*.

2.4.3. Antioxidant assay

In terms of radical scavenging ability, the antioxidant activity of the produced nanoparticles was determined using the stable radical DPPH (2,2-diphenyl-1-picryl-hydrazyl-hydrate). The nanoparticles were dissolved in DMSO at different concentrations. After that, 2.5ml of DPPH (0.1mM) DMSO solution was added to each concentration and allowed to stand for 30 minutes at 25°C. At 517nm, the absorbance of the samples was measured. The following formula was used to calculate the percentage of the DPPH scavenging effect.

$$(\%) \text{inhibition} = \left[\frac{\text{Abs of control} - \text{Abs of sample}}{\text{Abs of control}} \right] \times 100$$

2.4.4. Antileishmanial Assay (*Amastigotes* and *Promastigotes*):

Using a well-established procedure, green-produced ZnO-NPs were tested for antileishmanial activity against promastigotes and amastigotes of *Leishmania tropica*. *L.*

tropica (KWH23) strain-reared culture (10% FBS supplemented MI99 medium) of the parasite was used to test antileishmanial capabilities. The % inhibition was calculated as

$$\% \text{ Inhibition} = \left[1 - \left\{ \frac{\text{Absorbance of sample}}{\text{Absorbance of control}} \right\} \right] \times 100$$

2.5. Photo-catalytic Activity

For the photocatalytic activity of biosynthesized ZnO NPs nanoparticles, 10 ml of methylene blue (100ppm) stock solution was mixed with 10mg of nanoparticles, and the reaction combination was exposed to UV light. Centrifugation was performed to remove the catalyst from the sample, and the absorption peaks were evaluated with a UV-Visible spectrophotometer. The absorbance at a wavelength of 663nm was used to determine dye degradation in terms of concentration rise and reduction. The same procedure was applied for the methyl red dye degradation. The following formula was used to determine percent (%) degradation:

$$\% \text{ Degradation} = \left(\frac{A_i - A_f}{A_i} \right)$$

The initial absorbance of dye is A_i and the final absorbance of dyes after the catalyst's addition and exposure to UV light is A_f .

3. RESULTS

3.1. UV-visible spectra of ZnO Nanoparticle

Zinc Oxide nanoparticle synthesis was recognized through a gradual color change in the solution. The phytochemicals in *Spirogyra* aqueous extract were utilized as a reducing and capping agent and were primarily responsible for the bio-reduction of Zn^{2+} to ZnO ions. The spectrophotometer measurement was recorded at a scanning speed of 200-600nm. The λ -max was observed in the 280nm wavelength range (figure 1).

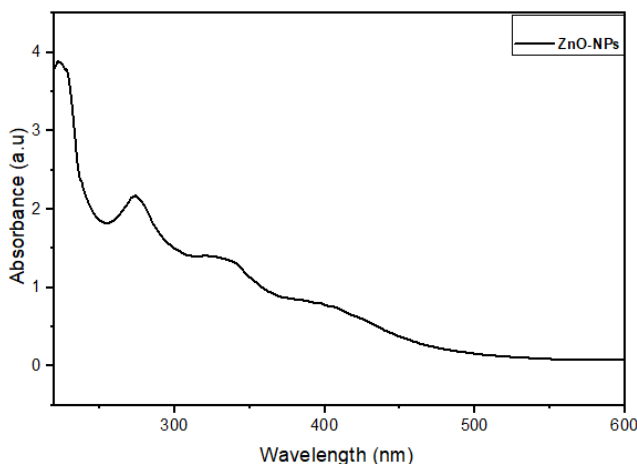


Figure 1: UV-Vis spectra of ZnO NPs using *Spirogyra* aqueous extract reveal characteristic absorption peaks at 280-600nm, demonstrating the successful synthesis

3.2. FTIR Analysis

To determine the functional groups involved in the capping and reduction of zinc nitrate to ZnO Nanoparticles, Fourier transform infrared spectroscopy was used within a wavelength range of 400-4000 cm^{-1} . Three significant peaks were identified at 3384 cm^{-1} , 1120 cm^{-1} , and 600 cm^{-1} (figure 2). These observed peaks line up with the stretching vibration of the O-H and C-H bonds in alcohols, alkenes, and alkanes, respectively. The FTIR results revealed phytochemicals in *Spirogyra* extract aligning with the zinc oxide nanoparticles. One transmission band due to a C-O bond was thus observed at 1633 cm^{-1} , respectively. The stretching band at 600 cm^{-1} (ZnO stretching vibration) confirmed the synthesis of ZnO particles [126,127].

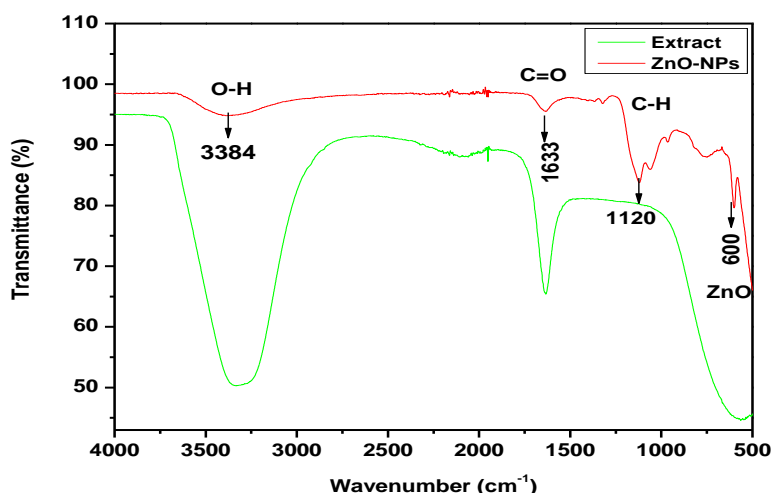


Figure 2: FT-IR spectra of *Spirogyra* Extract and ZnO-NP showing the characteristics of functional groups involved in reducing and capping bio-synthesized nanoparticles

3.3. EDX spectrum

By using EDX analysis, the elemental composition of produced zinc oxide nanoparticles was determined. The presence of zinc and oxygen signals in the ZnO Nanoparticles formed using *spirogyra* extract was confirmed by the EDX spectrum (figure 3). ZnO nanoparticles have a strong signal at 0.3 KeV (26%) and another signal at 1.1 KeV (20%). The presence of biomolecules in the *spirogyra* extract has generated additional signals in the EDX spectrum, which include signals for oxygen at 0.5 KeV (42 %), sulfur at 2.2 KeV (8.65 %), and potassium at 3.3 KeV (1.27 %).

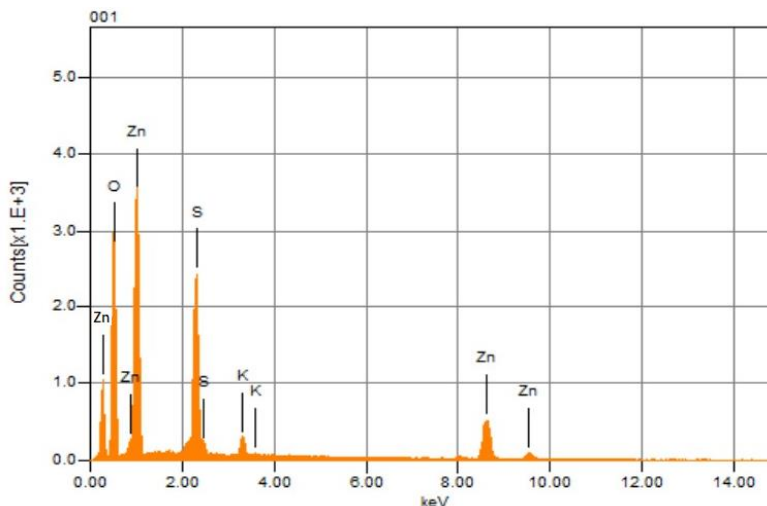


Figure 3: Energy-Dispersive X-ray Elemental studies of ZnO nanoparticles, showing the presence of Zn and O elements and confirming the formation of ZnO-NPs

3.4. SEM Analysis

The particle size and surface texture of the samples were morphologically analyzed through Scanning Electron Microscope (SEM). The SEM shows that the nanocrystals were irregular with homogenous morphology, agglomerated, well-dispersed, and with an average size of 52.96nm (figure 4).

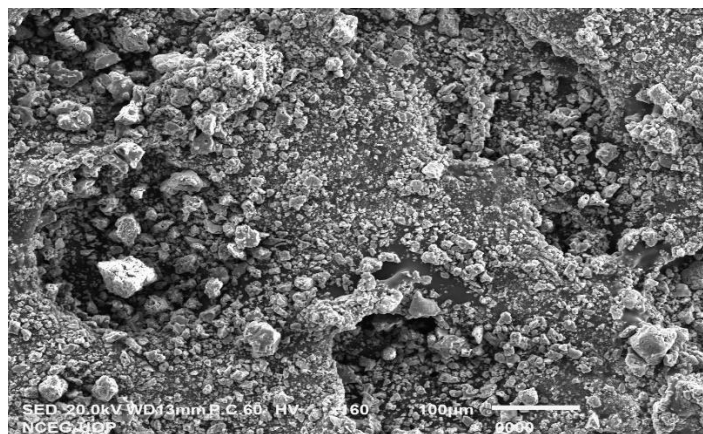


Figure 4: SEM Analysis of ZnO-NPs using *spirogyra* aqueous extract shows irregular with homogenous morphological properties

3.5. XRD Analysis

X-ray diffraction study was utilized to determine the nanoparticles' phase purity and crystal structure. Comparing the XRD diffractogram with the data from JCPDS card No. 89-1397 shows that the wurtzite structure is exceptionally well matched, and no indications of a phase structure or impurity peaks were observed. The diffraction peaks

are strong and compact, suggesting the product has a good crystalline nature. The presence of sharp, intense diffraction peaks at 31.76, 34.15, 37.24, 48.27, 58.18, 63.68, and 69.89 corresponding with those from (1 00), (0 02), (1 01), (102), (11 0), (1 03), (112) orientations, respectively (figure 5). The average crystallite size of the ZnO NPs is about 52.96 nm.

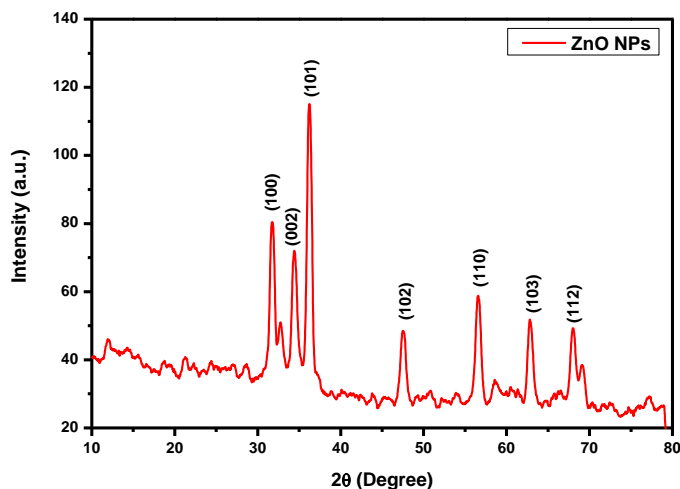


Figure 5: XRD Analysis of ZnO-NPs using *Spirogyra* aqueous extract, showing characteristic peaks and the average crystallite size of ZnO-NPs

3.6 Biological activities

3.6.1. Biocompatibility Studies

A biocompatibility study was performed on human red blood cells to demonstrate the biocompatibility of the green produced Nanoparticles. In this experiment, hemolysis of human red blood cells is observed in response to various nanoparticle concentrations (25-100 $\mu\text{g}/\text{mL}$). A spectrophotometer is used to evaluate RBC hemolysis at 405 nm. RBC hemolysis will be visible only if the sample has the capacity to disrupt the cells. According to the American Society for Testing Materials' criteria for biocompatibility of substances, substances with 2 >% hemolysis are labelled as nonhemolytic, 2-5% slightly hemolytic, and >5% are regarded hemolytic (Iqbal, et al. 2019). Even at high concentrations, all tester solutions of manufactured nanoparticles exhibit non-hemolysis, demonstrating their excellent biocompatibility. The phytochemically synthesized ZnO-NPs are hem-compatible even at an elevated concentration of 100 $\mu\text{g}/\text{mL}$ (table 1 & Figure 6).

Table 1: % Hemolysis of Green Synthesized ZnO-NPs

S. No	Conc. ($\mu\text{g}/\text{mL}$)	%hemolysis
1	100	0.98 \pm 0.12
2	75	0.67 \pm 0.13
3	50	0.46 \pm 0.08
4	25	0.13 \pm 0.07

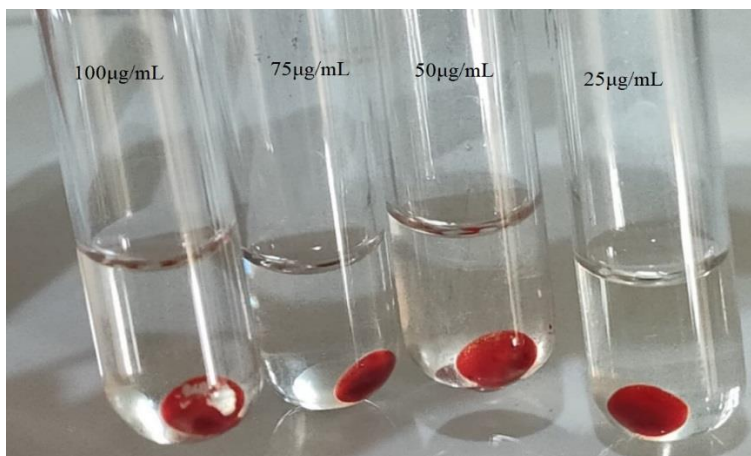


Figure 6: Hemolysis of biogenic ZnO NPs shows the extent of red blood cell lysis and indicates their potential cytotoxicity in biomedical applications

3.6.2. Antibacterial assay

Due to its high surface area-to-volume ratio, zinc oxide nanoparticles are exploited for their antibacterial properties. The antibacterial activity of ZnO-NPs, antibiotics, and their synergistic effect was evaluated using the disc diffusion method on agar plates against tested bacterial strains, i.e., *Acetobacter*, *B. Subtilis*, *Klebsiella pneumonia*, *P. Aeruginosa*, and *P. Vulgaris*. Variations in synergistic antibiotic activity were observed in the presence of ZnO Nanoparticles, with an increase in the zones of inhibition (figure 7a & 7b). When combined with ciprofloxacin, ZnO Nanoparticles demonstrate efficient activity against *K. pneumonia* and *B. subtilis* with a 30 ± 0.21 and 30 ± 0.26 mm zone of inhibition. In addition, ciprofloxacin coated ZnO NPs showed significant activity with an inhibition zone of 26.5 ± 0.34 against *P. vulgaris*.

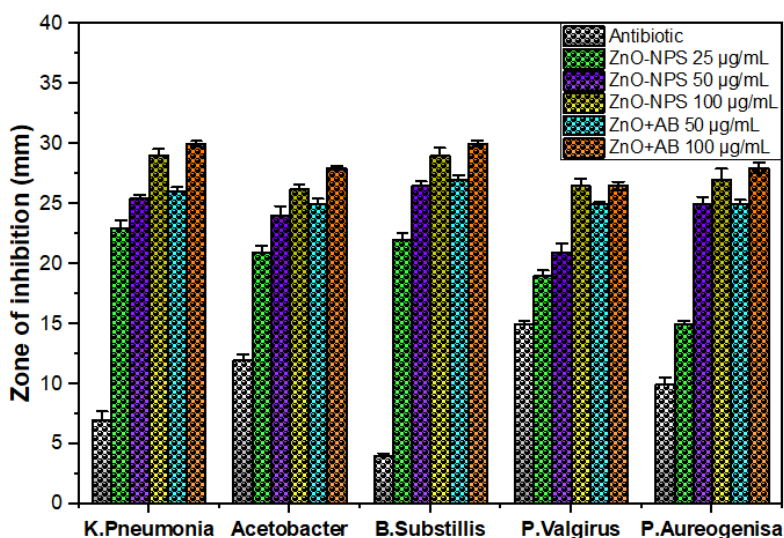


Figure 7a: Antibacterial activity of ZnO-NPs against pathogenic bacteria, displaying inhibition zones and indicating as a bactericidal agent

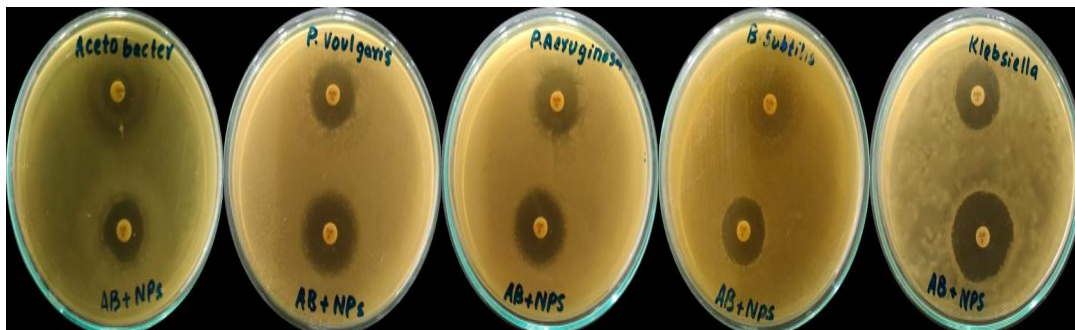


Figure 7b: Antibacterial activity of ZnO-NPs against Pathogenic Bacteria

3.6.3. Anti-leishmanial assay

An obligately intracellular parasite from *Leishmania* spp. causes leishmaniasis, a vector-borne infection (Reithinger, et al. 2007). Amphotericin B, miltefosine, pentamidine, and antimonial are a few drugs used to treat *Leishmania* in healthcare situations. Mild to severe toxic side effects of the medication, including cardiotoxicity, pancreatitis, renal failure, and anemia, complicate the therapy (Karimkhani, et al. 2016). The biocompatible ZnO nanoparticles demonstrate outstanding antileishmanial efficacy against both amastigotes and promastigotes ($78\% \pm 0.65$ and $80\% \pm 0.166$, respectively) when compared to the standard treatment of Amphotericin B (88 and 94% at 100 g/mL) (figure 8a & 8b).

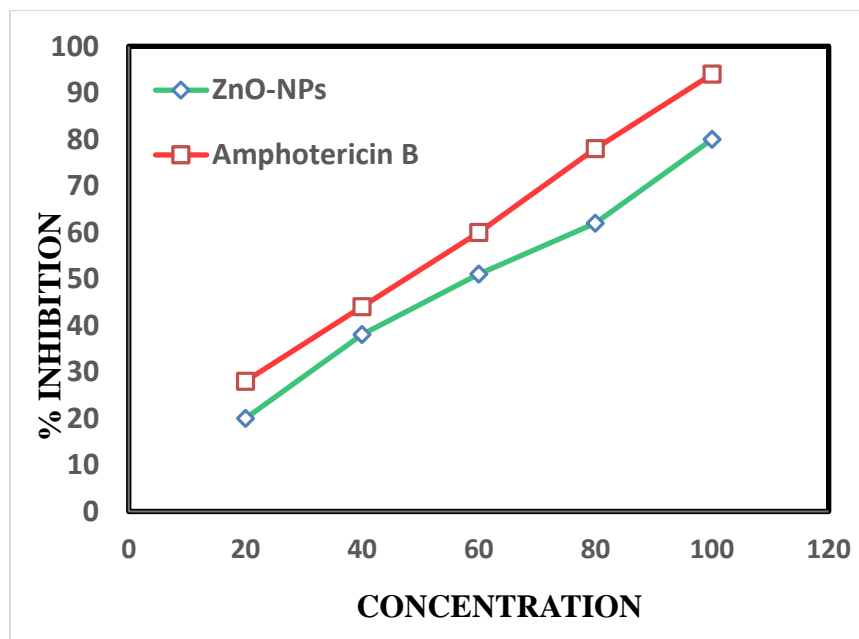


Figure 8a: Antileishmanial activity of ZnO-NPs against promastigote parasite

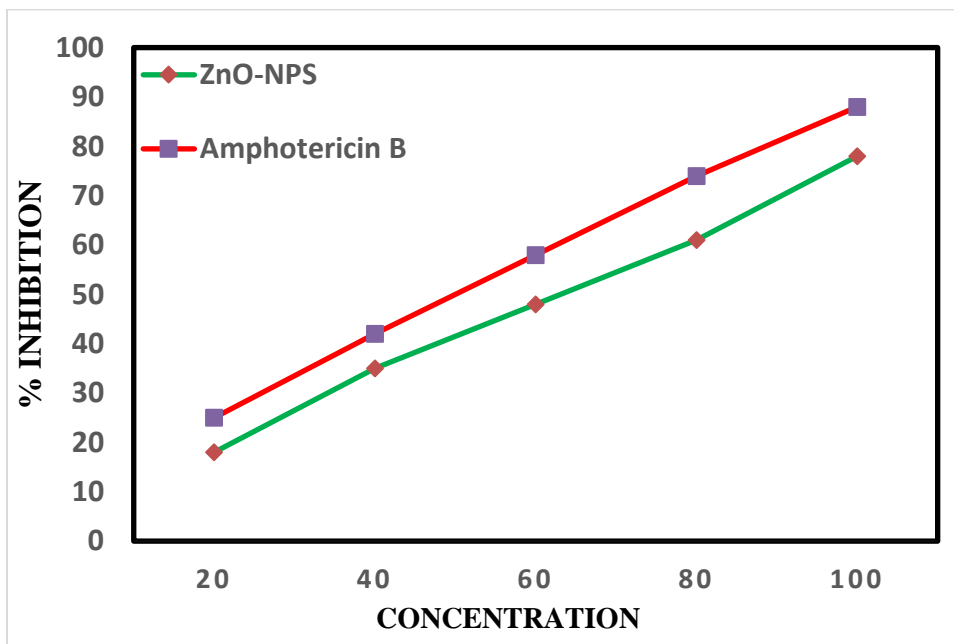


Figure 8b: Antileishmanial activity of ZnO-NPs against Amastigotes parasite

3.6.4. Antioxidant assay

To evaluate the antioxidant potential of the phytochemically synthesized ZnO-NPs, a DPPH free radical scavenging assay was used with ascorbic acid as the standard. The synthesized ZnO nanoparticles demonstrated effective activity when compared to standard ascorbic acid. As indicated in Figure 9, ZnO nanoparticles (81.10±0.26) at 100µg/ml demonstrated the highest free radical scavenging effect compared to ascorbic acid (96.21±0.88).

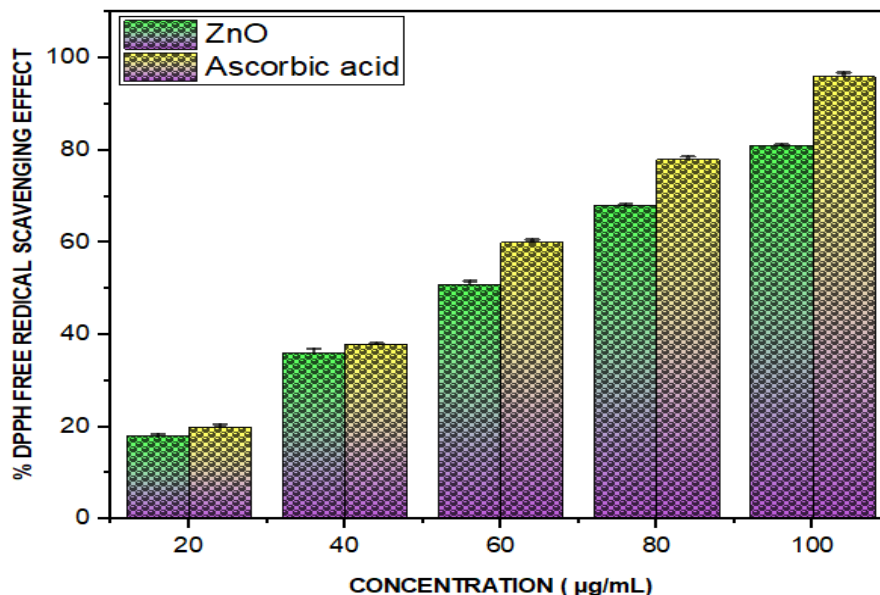


Figure 9: DPPH free radicals scavenging activity of ZnO-NPs using Spirogyra extract

3.7. Dye degradation activity

The phytochemically synthesized ZnO nanoparticles showed remarkable photocatalytic activity against MB (methylene blue) and MR (methyl red) dyes (10a & 11a). Within 10 minutes of the photocatalysis, 43% of the total MB concentration was degraded, with a final methylene blue dye removal efficacy of 84% at 60 minutes. The dye degradation kinetics was characterized by an initial quick phase followed by a slow secondary phase. The amphoteric potential of the biologically synthesized ZnO nanoparticles for photocatalytic degradation of both synthetic dyes was evaluated. A significant decrease in the predominant absorption peak of MR within the first 10 minutes was observed. Within 5 minutes of the photocatalysis, around 80% of methyl red dye was degraded, with a final MR degradation efficiency of 95% at 60 minutes.

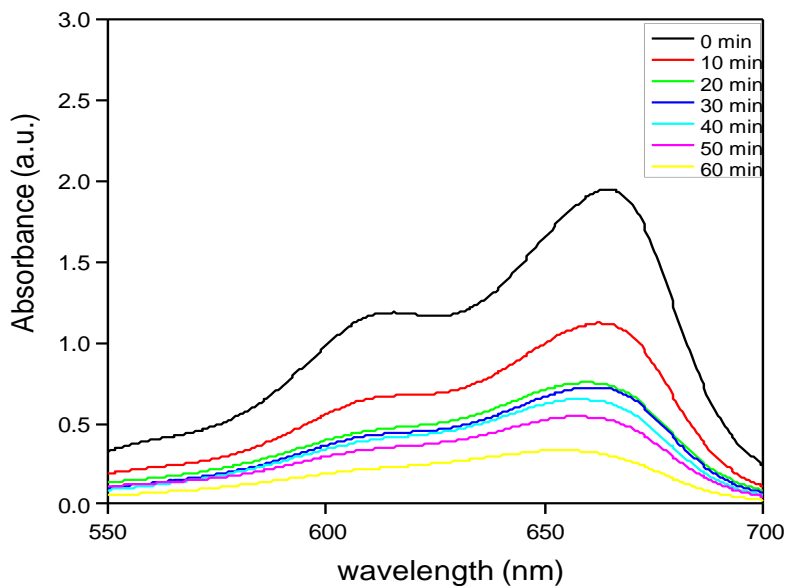


Figure 10a: UV-VIS spectra of Methylene blue (MB) dye degradation by ZnO-NPs

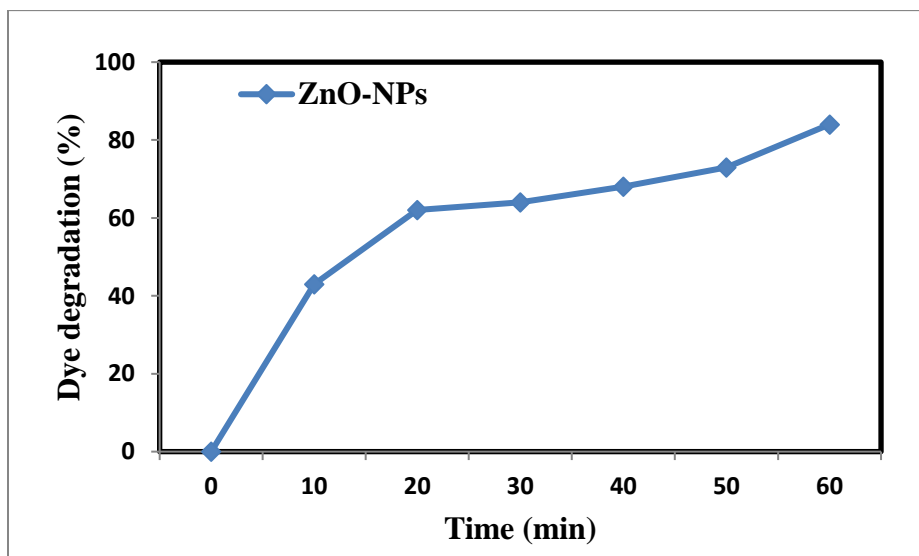


Figure 10b: Percentage Degradation of Methylene blue (MB) dye by ZnO-NPs

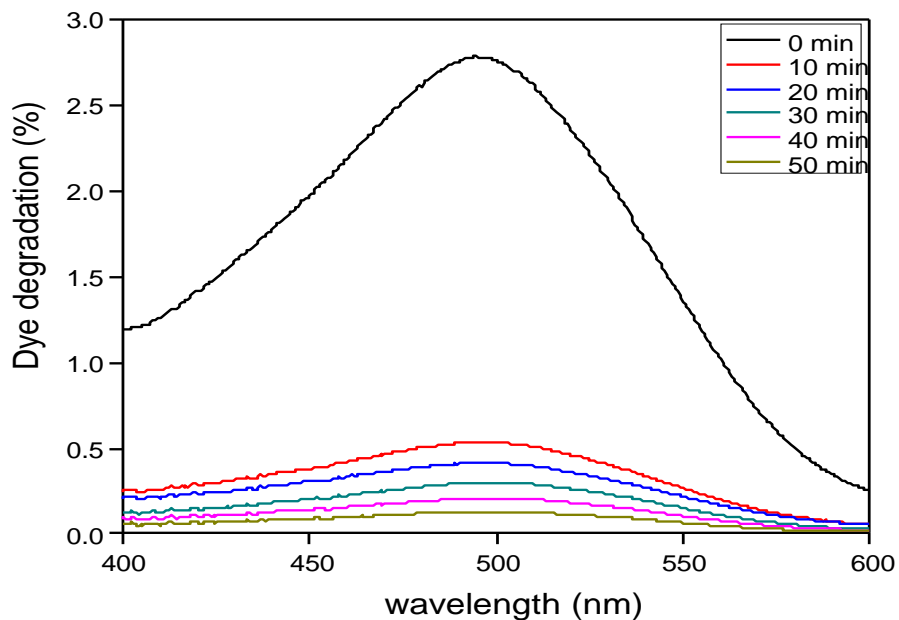


Figure 11a: UV-VIS spectra of Methyl red (MR) dye degradation by ZnO-NPs

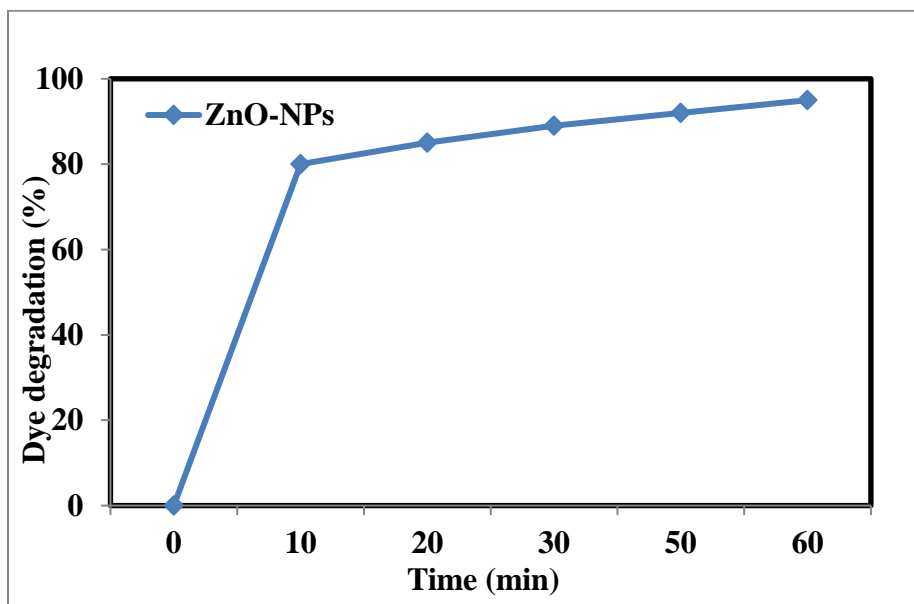


Figure 11b: Percentage Degradation of Methylene Red (MR) dye by ZnO-NPs

4. DISCUSSION

Nanotechnology has applications in diverse fields, where biological systems are used to synthesize nanoparticles due to numerous advantages over physical and chemical approaches. Plants are excellent resources for producing metal NPs. Zinc oxide nanoparticles were synthesized in the present study using *Spirogyra* aqueous extract.

Other related research has revealed other plant and algal extracts, such as Punica granatum peel extract (Mishra and Sharma 2015), the leaf extract of Hibiscus subdariffa *Tetraselmis indica* (algae) for the synthesis of ZnO NPs (Bala, et al. 2015).

In the present work, ZnO NPs were characterized using a variety of approaches. UV-Vis's absorbance in the 280 nm region initially confirmed the synthesis of ZnO NPs. *Ixora coccinea* leaf extract was used in another investigation to synthesize zinc oxide nanoparticles, which had an absorbance peak at 340 nm (Yedurkar, et al. 2016). FTIR analysis of Spirogyra aqueous extract-mediated ZnO nanoparticles showed interrelation and vibrations of different functional groups, i.e., alkanes, alcohols, aromatics, and alkenes, which were the stretching vibration peaks of ZnO NPs. Previously similar results reported that the peaks were due to $-C = O-$, $O-H$, and $C-H$ stretching vibrations, respectively (Yedurkar, et al. 2016)[22].

The EDX of ZnO nanoparticles revealed peaks for zinc atoms at 1 keV and 9 keV and for oxygen atoms at 0.5 keV with weight percentages of Zn at 55.92% and oxygen at 44.08% (Davar, et al. 2015). The morphology of the produced ZnO nanoparticles was examined using SEM analysis, indicating that the particles are agglomerated, irregular, and homogenous. In a previous study, green synthesized ZnO nanoparticles using aloe vera broth extract were homogenous and agglomerated with a particle size in the range of 25-55 nm (Gnanasangeetha and SaralaThambavani 2013). X-Ray Diffractometer confirmed the presence of Zn, oxygen, and other elements (Vidya, et al. 2013). Induced hemolysis is a simple and effective method to evaluate nanoparticle biocompatibility. All substances entering the bloodstream come into contact with the red blood cells (RBCs). According to the current study, phytochemically produced ZnO nanoparticles are non-hemolytic and biocompatible for medical applications (Haque, et al. 2022).

Microorganisms poses a significant threat to the public's health (Prasad, et al. 2021). The phytochemically synthesized ZnO NPs have strong antibacterial activity against many Gram-negative and Gram-positive bacterial strains. In the current study, spirogyra-mediated green synthesized ZnO Nanoparticles showed excellent antibacterial activity against several harmful bacterial strains. The synergistic effect of ZnO NPs and antibiotics performed effectively to enhance the antibacterial effect. This combinational therapy may be further evaluated to create novel formulations of ZnO Nanoparticles in conjunction with antibiotics since the combined effect of antibiotics and ZnO NPs will make it harder for harmful bacteria to develop acquired immunity.

Highly reactive molecules known as free radicals are produced throughout the daily activities of organisms and during the conversion of food into energy. Additionally, the body is exposed to free radicals from external sources, including smoke, air pollution, and sun exposure. These harmful free radicals can damage DNA, cell walls, and other cellular components (DNA). The creation and removal of free radicals are balanced in a cell. Excessive exposure to free radicals can result in oxidative stress, a state in cells that can lead to a variety of diseases like cancers, cardiovascular disease, liver problems, etc. (Aseervatham, et al. 2013). The antioxidants reduce oxidative stress, through a pathophysiological reaction brought on by an imbalance between the ability of

endogenous antioxidants and the production of oxidants to counteract them (Khalil, et al. 2019). The inherent redox activity of metal oxide nanoparticles is strongly associated with radical trapping, as well as superoxide dismutase- and catalase-like activities. Antioxidants play a critical role in the organisms' defense against diseases associated with the attack of free radicals (Pisoschi and Negulescu 2011). The significant DPPH free radical scavenging potential (81.10 %) was observed at a 100 g/ml Zinc Oxide nanoparticles (Bailey, et al. 2019).

Leishmaniasis is a disease that goes untreated and affects people in poverty in approximately 100 countries. The present therapy methods are inefficient, expensive, and linked to significant toxic effects, making treating and controlling this disease more difficult (Croft and Coombs 2003). ZnO NPs were utilized in the current study to effectively treat the Leishmania parasite. Our results are consistent with a recent work that discovered ZnO produced using *Sageretia Thea* extract strongly inhibiting the promastigote and amastigote forms of *L. tropica* (Praveen Kumar and Bhat Sumangala 2012).

Over 7×10^5 tons of synthetic dyes are manufactured annually globally. Every year, the textile sector releases up to 200,000 tons of these harmful dyes into the environment by releasing industrial effluents (Prasad, et al. 2021). These harmful dyes increase the biochemical and chemical oxygen demand (BOD and COD), causes photosynthesis impairment, plant growth suppression, entrance into the food chain, recalcitrant and bioaccumulation requirements, and potential enhancement of toxicity, mutagenicity, and carcinogenicity. ZnO has high photodegradation efficiency and may be employed in large-scale wastewater treatment. Organic pollutants (dyes) are the most studied in dye degradation due to their abundant discharge in industrial effluents with substantial environmental effects. ZnO NPs synthesized using conventional chemical approaches and green methods have been established as photocatalysts for the dye degradation of various water contaminants under UV light. ZnO nanoparticles showed excellent degradation against both the MB and MR dyes (Fu and Fu 2015).

References

1. Aseervatham GSB, Sivasudha T, Jeyadevi R, Arul Ananth D (2013). Environmental factors and unhealthy lifestyle influence oxidative stress in humans—an overview. *Environmental Science and Pollution Research* 20:4356-4369
2. Asha AB, Narain R (2020) Nanomaterials properties. In: *Polymer science and nanotechnology*. Elsevier, pp 343-359
3. Bailey F, Mondragon-Shem K, Haines LR, Olabi A, Alorfi A, Ruiz-Postigo JA, Alvar J, Hotez P, Adams ER, Velez ID (2019). Cutaneous leishmaniasis and co-morbid major depressive disorder: a systematic review with burden estimates. *PLoS neglected tropical diseases* 13:e0007092
4. Bala N, Saha S, Chakraborty M, Maiti M, Das S, Basu R, Nandy P (2015). Green synthesis of zinc oxide nanoparticles using *Hibiscus subdariffa* leaf extract: effect of temperature on synthesis, anti-bacterial activity and anti-diabetic activity. *RSC Advances* 5:4993-5003
5. Cai G, Yan P, Zhang L, Zhou H-C, Jiang H-L (2021). Metal-organic framework-based hierarchically porous materials: synthesis and applications. *Chemical Reviews* 121:12278-12326

6. Chanda S, Dave R, Kaneria M, Nagani K (2010). Seaweeds: a novel, untapped source of drugs from sea to combat infectious diseases. *Current research, technology and education topics in applied microbiology and microbial biotechnology* 1:473-480
7. Chiang WH, Mariotti D, Sankaran RM, Eden JG, Ostrikov K (2020). Microplasmas for advanced materials and devices. *Advanced Materials* 32:1905508
8. Croft SL, Coombs GH (2003). Leishmaniasis—current chemotherapy and recent advances in the search for novel drugs. *Trends in parasitology* 19:502-508
9. Davar F, Majedi A, Mirzaei A (2015). Green synthesis of ZnO nanoparticles and its application in the degradation of some dyes. *Journal of the American Ceramic Society* 98:1739-1746
10. Fu L, Fu Z (2015). Plectranthus amboinicus leaf extract–assisted biosynthesis of ZnO nanoparticles and their photocatalytic activity. *Ceramics International* 41:2492-2496
11. Gnanasangeetha D, SaralaThambavani D (2013). One pot synthesis of zinc oxide nanoparticles via chemical and green method. *Res J Mater Sci* 2320:6055
12. Haque S, Faidah H, Ashgar SS, Abujamel TS, Mokhtar JA, Almuhayawi MS, Harakeh S, Singh R, Srivastava N, Gupta VK (2022). Green Synthesis of Zn (OH) 2/ZnO-Based Bionanocomposite using Pomegranate Peels and Its Application in the Degradation of Bacterial Biofilm. *Nanomaterials* 12:3458
13. Iqbal J, Abbasi BA, Mahmood T, Kanwal S, Ahmad R, Ashraf M (2019). Plant-extract mediated green approach for the synthesis of ZnONPs: Characterization and evaluation of cytotoxic, antimicrobial and antioxidant potentials. *Journal of Molecular Structure* 1189:315-327
14. Jeyaraj M, Gurunathan S, Qasim M, Kang M-H, Kim J-H (2019). A comprehensive review on the synthesis, characterization, and biomedical application of platinum nanoparticles. *Nanomaterials* 9:1719
15. Karimkhani C, Wanga V, Coffeng LE, Naghavi P, Dellavalle RP, Naghavi M (2016). Global burden of cutaneous leishmaniasis: a cross-sectional analysis from the Global Burden of Disease Study 2013. *The Lancet Infectious Diseases* 16:584-591
16. Khalil I, Yehye WA, Etxeberria AE, Alhadi AA, Dezfooli SM, Julkapli NBM, Basirun WJ, Seyfoddin A (2019). Nanoantioxidants: Recent trends in antioxidant delivery applications. *Antioxidants* 9:24
17. Mishra V, Sharma R (2015). Green synthesis of zinc oxide nanoparticles using fresh peels extract of *Punica granatum* and its antimicrobial activities. *International Journal of Pharma Research and Health Sciences* 3:694-699
18. Mohamed S, Hashim SN, Rahman HA (2012). Seaweeds: A sustainable functional food for complementary and alternative therapy. *Trends in Food Science & Technology* 23:83-96
19. Pisoschi AM, Negulescu GP (2011). Methods for total antioxidant activity determination: a review. *Biochem Anal Biochem* 1:106
20. Pramanik P, Krishnan P, Maity A, Mridha N, Mukherjee A, Rai V (2020). Application of nanotechnology in agriculture. *Environmental Nanotechnology Volume 4* 317-348
21. Prasad AR, Williams L, Garvasis J, Shamsheera K, Basheer SM, Kuruvilla M, Joseph A (2021). Applications of phyto-genic ZnO nanoparticles: A review on recent advancements. *Journal of Molecular Liquids* 331:115805
22. Praveen Kumar G, Bhat Sumangala K (2012). Decolorization of azo dye Red 3BN by bacteria. *International Research Journal of Biological Sciences* 1:46-52
23. Reithinger R, Dujardin J-C, Louzir H, Pirmez C, Alexander B, Brooker S (2007). Cutaneous leishmaniasis. *The Lancet infectious diseases* 7:581-596

24. Shafey AME (2020). Green synthesis of metal and metal oxide nanoparticles from plant leaf extracts and their applications: A review. *Green Processing and Synthesis* 9:304-339
25. Singh P, Katare RK (2019). A Study on effect of zinc oxide and silver nanoparticles in Bio Physics.
26. Soto-Robles C, Luque P, Gómez-Gutiérrez C, Nava O, Vilchis-Nestor A, Lugo-Medina E, Ranjithkumar R, Castro-Beltrán A (2019). Study on the effect of the concentration of Hibiscus sabdariffa extract on the green synthesis of ZnO nanoparticles. *Results in Physics* 15:102807
27. Thi TUD, Nguyen TT, Thi YD, Thi KHT, Phan BT, Pham KN (2020). Green synthesis of ZnO nanoparticles using orange fruit peel extract for antibacterial activities. *RSC advances* 10:23899-23907
28. Tyagi D, Wang H, Huang W, Hu L, Tang Y, Guo Z, Ouyang Z, Zhang H (2020). Recent advances in two-dimensional-material-based sensing technology toward health and environmental monitoring applications. *Nanoscale* 12:3535-3559
29. Vidya C, Hiremath S, Chandraprabha M, Antonyraj M, Gopal IV, Jain A, Bansal K (2013). Green synthesis of ZnO nanoparticles by *Calotropis gigantea*. *Int J Curr Eng Technol* 1:118-120
30. Yedurkar S, Maurya C, Mahanwar P (2016). Biosynthesis of zinc oxide nanoparticles using ixora coccinea leaf extract—a green approach. *Open Journal of Synthesis Theory and Applications* 5:1-14
31. Zhang G-X, Reilly AM, Tkatchenko A, Scheffler M (2018). Performance of various density-functional approximations for cohesive properties of 64 bulk solids. *New Journal of Physics* 20:063020
32. Zhang X-F, Liu Z-G, Shen W, Gurunathan S (2016). Silver nanoparticles: synthesis, characterization, properties, applications, and therapeutic approaches. *International journal of molecular sciences* 17:1534
33. Zuercher AW, Fritsche R, Corthésy B, Mercenier A (2006). Food products and allergy development, prevention and treatment. *Current opinion in biotechnology* 17:198-203